International Journal of Thermophysics, Vol. 11, No. 2, 1990

Thermophysical Properties of Ice, Snow, and Sea Ice[1]

S. Fukusako[2]

The paper reviews and discusses data and information on the thermophysical properties of ice, snow, and sea ice. These properties include thermal conductivity, specific heat, density, thermal diffusivity, latent heat of fusion, thermal expansion, and absorption coefficient. The available data are shown graphically for convenience in conjunction with the recommended correlation equations.

KEY WORDS: absorption coefficient; density; ice; latent heat of fusion; sea ice; snow; specific heat; thermal conductivity; thermal diffusivity; thermal expansion.

1. INTRODUCTION

Engineering in cold regions has recently received increased interest, due mainly to petroleum exploration and related activities which include the design and construction of roads, airfields, pipelines, and numerous types of structures. Arctic or cold environments provide a variety of unique freezing or melting phenomena in water, air, earth, and biological fields. The thermal interaction of these engineering systems with the environment results in unexpected failures of the system. These failures are usually based on utilizing the technology developed in mild-temperature climates without considering the special conditions and problems of the cold climates.

For cold-regions technology, the thermophysical properties of ice, snow, and sea ice are needed. For instance, a knowledge of the thermal expansion coefficient of sea ice is markedly needed to solve a variety of ice-engineering problems: in estimating thermal ice pressure on offshore Arctic

[1] Paper presented at the Second U.S.–Japan Joint Seminar on Thermophysical Properties, June 23, 1988, Gaithersburg, Maryland, U.S.A.

[2] Department of Mechanical Engineering, Hokkaido University, Sapporo 060, Japan.

0195-928X/90/0300-0353$06.00/0

structures and in studying thermal cracking and weakening of sea-ice sheets.

The principal objective of this work is to review and discuss available data and information on thermophysical properties of ice, snow, and sea ice. In Section 2, studies of thermal conductivity, specific heat, density, thermal diffusivity, latent heat of fusion, thermal expansion, and absorption coefficient of ice are reported. In the values of thermal conductivity of ice, some scatter is observed. At the temperatures of practical interest in cold climates, the cubic expansion coefficient is well expressed as a linear function of temperature. In Section 3, the thermal conductivity, specific heat of snow, and thermal diffusivity of snow over a large range of temperature are reviewed. A much greater scatter is observed in the values of thermal conductivity of snow. Reproducible data for snow are much more difficult to obtain because of the effects of water-vapor diffusion on the temperature field and the mass redistribution within a snow layer. A study of thermophysical properties of sea ice is given in Section 4. It is demonstrated that the thermophysical properties are functions of both salinity and temperature.

2. THERMOPHYSICAL PROPERTIES OF ICE

2.1. Thermal Conductivity of Ice

Measurements of the thermal conductivity of ice made prior to 1958 have been reviewed by Powell [1]. Landauer and Plumb [2] pointed out that there were no considerable differences among the thermal conductivities of laboratory-grown single crystals, glacial single crystals, and commercial polycrystalline ice, although the thermal conductivity value parallel to the c-axis of the single crystals may be about 5% greater than that normal to the c-axis.

Figure 1 shows that thermal conductivity data for polycrystalline ice obtained by Jakob and Erk [3], Landauer and Plumb [2], Powell [1], Ratcliffe [4], Dillard and Timmerhaus [5], Ashworth [6], and Sakazume and Seki [7]. Variations among the reported data appear to be due to the different techniques and conditions such as sample preparation, sample purity, measurement method, and reproducibility of experimental data. The measured values at 273.15 K (0°C) and atmospheric pressure are $2.20\,W \cdot m^{-1} \cdot K^{-1}$ by Schofield and Hall [8] and Ratcliffe [4], $2.09\,W \cdot m^{-1} \cdot K^{-1}$ by Van Dusen [9], $2.23\,W \cdot m^{-1} \cdot K^{-1}$ by Jacob and Erk [3], anbd $2.26\,W \cdot m^{-1} \cdot K^{-1}$ by Dillard and Timmerhaus [5]. For

practical purposes, it was suggested by Sakazume and Seki [7] that one can use

$$\lambda_i = 1.16(1.91 - 8.66 \times 10^{-3}\theta + 2.97 \times 10^{-5}\theta^2) \quad (\mathrm{W \cdot m^{-1} \cdot K^{-1}};\ \theta,\ ^\circ\mathrm{C}) \qquad (1)$$

to calculate λ_i at temperatures ranging from 100 to 273 K.

The thermal conductivity of ice at temperatures below 100 K was determined by Klinger [10], whose data are shown in Fig. 2 along with those obtained by Ratcliffe [4], Dean and Timmerhaus [11], and Ashworth [6]. Klinger's data indicate clearly that the thermal conductivity of ice increases with decreasing temperature, passes through a maximum at about 7 K, and then decreases as the temperature decreases furthermore.

2.2. Specific Heat of Ice

Reviews and summaries of the many measurements of the specific heat of ice made in the early twentieth century have been reported by Dickinson and Osborne [12] and Dorsey [13]. Giauque and Stout [14] measured the specific heat of hexagonal ice between 15 and 273 K. Heat capacity

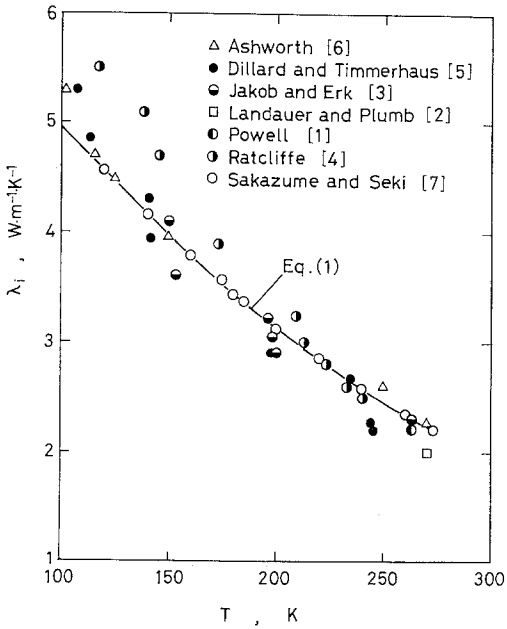

Fig. 1. Thermal conductivity of ice in the range 100–300 K.

measurements for hexagonal ice at very low temperatures ranging from 2 and 27 K were carried out by Flubacher et al. [15]. Sugisaki et al. [16] determined the specific heats of amorphous, cubic, and hexagonal ice between 20 and 250 K. Sakazume and Seki [7], using the Krisher method, made extensive measurements of the volumetric specific heat of ice $(\rho C_p)_i$ at temperatures from 110 to 273 K.

Figure 3 shows the experimental C_{p_i} data for hexagonal and cubic ice. The data can be represented by

$$C_{p_i} = 0.185 + 0.689 \times 10^{-2}\, T \quad (\mathrm{kJ \cdot kg^{-1} \cdot K^{-1}}), \quad 273\ \mathrm{K} \geqslant T \geqslant 90\ \mathrm{K} \tag{2}$$

$$C_{p_i} = 0.895 + 10^{-2}\, T \quad (\mathrm{kJ \cdot kg^{-1} \cdot K^{-1}}), \quad 90\ \mathrm{K} \geqslant T \geqslant 40\ \mathrm{K} \tag{3}$$

Flubacher et al. [15] determined the specific heat of ice at extremely low temperatures (near 0 K) and found that the relationship between C_{p_i} and T was not linear between 0 and 15 K.

2.3. Density of Ice

The density of pure ice has been determined by a number of investigators. Based on a review of numerous measurements. Dorsey [13]

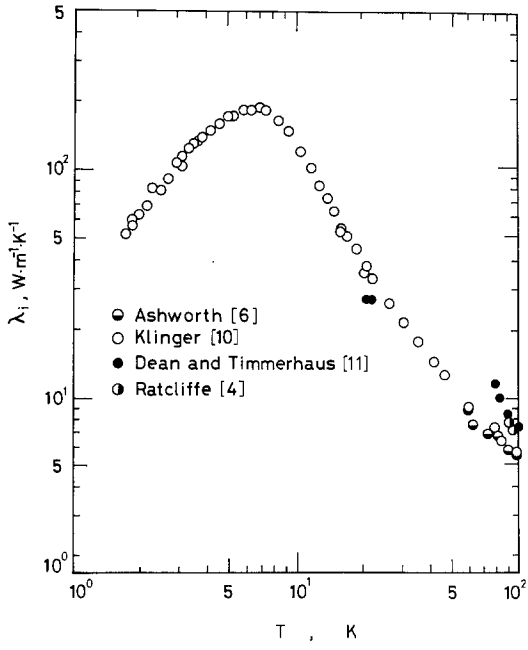

Fig. 2. Thermal conductivity of ice below 100 K.

pointed out that the bulk density of ice at 0°C is varied from 916 to 918 $kg \cdot m^{-3}$. Ginnings and Corruccini [17] reported a value of $916.71 \pm 0.05\ kg \cdot m^{-3}$ at 0°C, which is in good agreement with the value of $916.4\ kg \cdot m^{-3}$ at 0°C given by Lonsdale [18]. Dandtl and Gregora [19] found that the density of ice decreases as it ages and that it may fluctuate by as much as 0.3% depending upon the conditions of growth.

Figure 4 shows ρ_i data which were deduced by Lonsdale [18] from the average of several diffraction measurements made prior to 1958, deduced by Eisenberg and Kauzmann [20] from X-ray diffraction measurements made by LaPlaca and Post [21], and deduced by Hobbs [22] from X-ray diffraction measurements made by Brill and Tippe [23]. The dashed line is due to Pounder [24]. Hobbs [22] concluded that at lower temperatures the data of LaPlaca and Post [21] and Brill and Tippe [23] were more reliable. The data for ρ_i can be represented by

$$\rho_i = 917(1 - 1.17 \times 10^{-4}\,\theta) \quad (kg \cdot m^{-3}), \qquad 0°C \geqslant \theta \geqslant -140°C \tag{4}$$

$$\rho_i = 930(1 - 1.54 \times 10^{-5}\,\theta) \quad (kg \cdot m^{-3}), \quad -140°C \geqslant \theta \geqslant -260°C \tag{5}$$

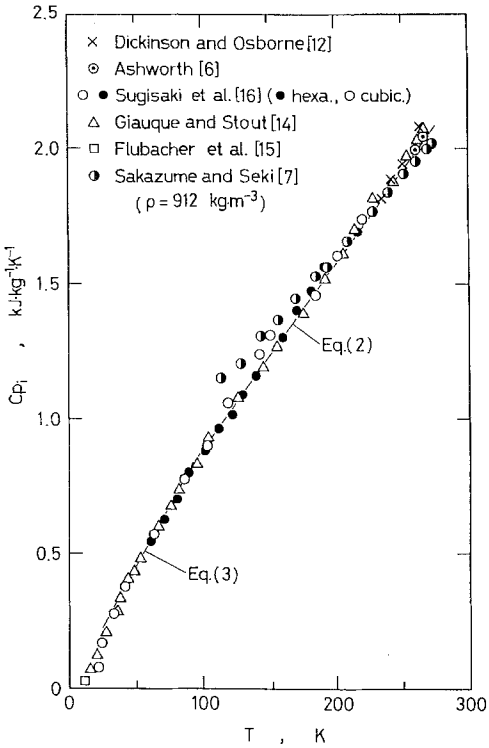

Fig. 3. Specific heat of ice.

2.4. Thermal Diffusivity of Ice

Cameron and Bull [25] obtained a value for the thermal diffusivity of Antarctic ice using the cyclic heating method and they obtained an average value of $(15.4 \pm 0.9)10^{-7}\,m^2 \cdot s^{-1}$ at about 253 K. James [26] determined the thermal diffusivity of artificial single crystals of ice parallel to the c-axis. The a_i values for the temperature of 100 to 273 K were measured by Sakazume and Seki [7] with the aid of Krisher's method.

2.5. Latent Heat of Fusion of Ice

The latent heat of fusion of ice L_{fi} is defined as the change in enthalpy as a unit mass of ice is converted isothermally and reversibly into water. Measurements of the latent heat of fusion of ice determined prior to 1925 were reviewed by Smith [27] and those up to 1940 by Dorsey [13]. The values reported for the latent heat of fusion of ice at 273.15 K (0°C) and atmospheric pressure are $333.9\,kJ \cdot kg^{-1}$ by Dickinson and Osborne [12], $333.6\,kJ \cdot kg^{-1}$ by Smith [27], and $333.5\,kJ \cdot kg^{-1}$ by Rossini et al. [28], respectively. Focrand and Gay (Hobbs [22]) based on determinations by Dickinson and Osborne [12] indicated that the latent heat of fusion of ice may decrease monotonically with a decrease in temperature.

2.6. Thermal Expansion

There are two kinds of thermal expansion coefficients. The coefficient of linear expansion α_l is a measure of the fractional change in length per

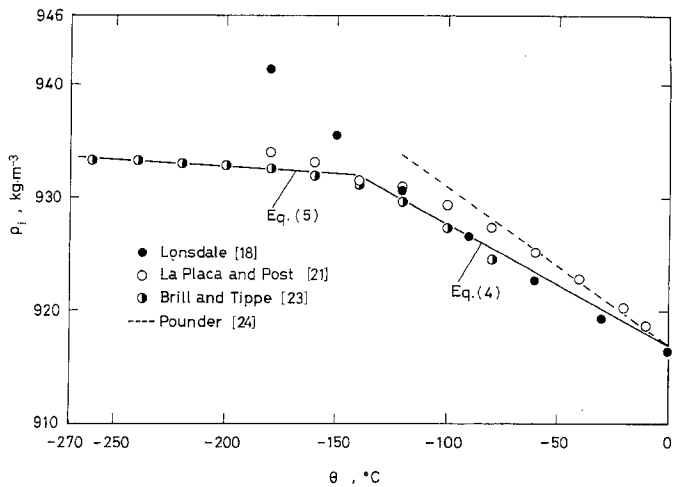

Fig. 4. Density of ice.

unit change in temperature. On the other hand, the coefficient of cubic expansions α_v is defined as the fractional change in volume per degree change in temperature.

The coefficients of thermal expansion of bulk ice at atmospheric pressure were determined by Jakob and Erk [29] for polycrystals, by Hamblin (Powell [1]) for single crystals both parallel to the c-axis and perpendicular to the c-axis, by Butkovich [30] for single crystals, and by Dantl [31] for single crystals. All experiments indicate that the coefficient of linear expansion decreases with a decrease in temperature. For the value α_{li} at 0°C, Butkovich [30] gave 52.92×10^{-6} (T^{-1}) for single crystals parallel to the c-axis, 52.33×10^{-6} (T^{-1}) for single crystals normal to the c-axis, and 52.33×10^{-6} (T^{-1}) for polycrystalline normal to the c-axis, respectively. Hamblin (Powell [1]) indicated that the coefficients of linear expansion of ice parallel to the c-axis were about 1.8 and 10% greater than those perpendicular to the c-axis at 273 and 73 K, respectively. Furthermore, Jakob and Erk [29] and Dantl [31] reported that ice has a negative coefficient of linear expansion below about 73 K.

The values for the coefficients of cubical expansion α_{vi} at atmospheric pressure are presented in Fig. 5, showing the data deduced by Leadbetter [32] from linear expansion coefficients given by Powell [1] and Dantl [31], deduced by Eisenberg and Kauzmann [20] from measurements of the unit-cell parameters made by LaPlaca and Post [21], and deduced by Hobbs [22] from measurements of the unit-cell parameters made by Brill and Tippe [23] (two α_{vi} data at mean temperatures of 183 and 163 K were

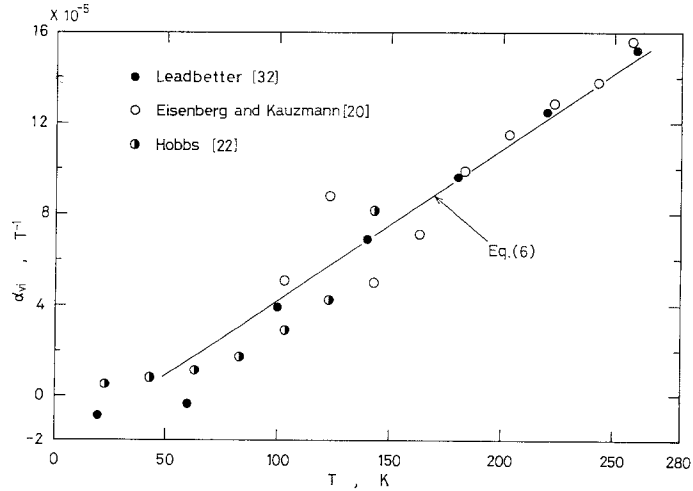

Fig. 5. Coefficient of cubic expansion of ice.

deleted). From Fig. 5 it is evident that α_{vi} increases generally with an increase in temperature, although there are some discrepancies among the three set of data. Yen [33] gave an expression for α_{vi} as

$$\alpha_{vi} = (0.67T - 24.86) \times 10^{-6} \quad (K^{-1}) \tag{6}$$

which appears to be adequate to calculate α_{vi} for engineering applications.

2.7. Absorption Coefficient of Ice

Irvine and Pollack [34] reviewed and evaluated the data reported up to 1968 for wavelengths longer than 0.95 μm. Absorption coefficients for clear ice in the spectral region 0.3 to 3 μm were reviewed by Goodrich [35]. Seki et al. [36] determined experimentally the k_v values for wavelengths between 0.3 and 2.5 μm using an ice layer 1 to 100 mm in thickness. The results are shown in Figs. 6 and 7. The figures show that the absorption coefficient of ice is a strong function of the wavelength. For visible wavelengths of 0.4 to 0.7 μm ice behaves approximately as a transparent medium. In the infrared region (0.7–30 μm), a number of absorption lines are present, resulting in quite large values of k_v, so that ice is essentially opaque. On the other hand, the absorption coefficient decreases to a great extent as the wavelength increases further over 100 μm (in the range of microwave and radiowave).

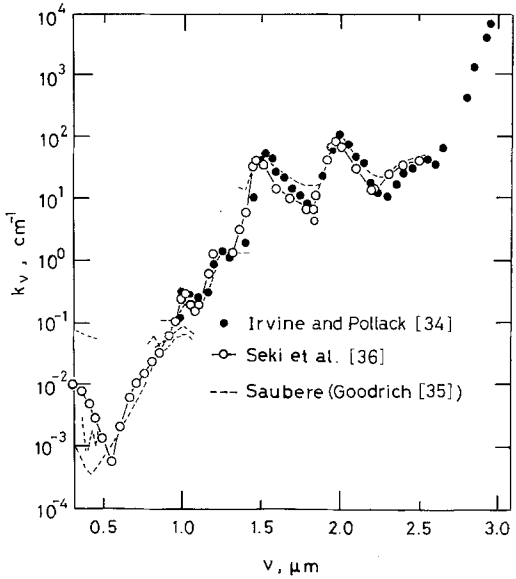

Fig. 6. Absorption coefficient of ice for short wavelength.

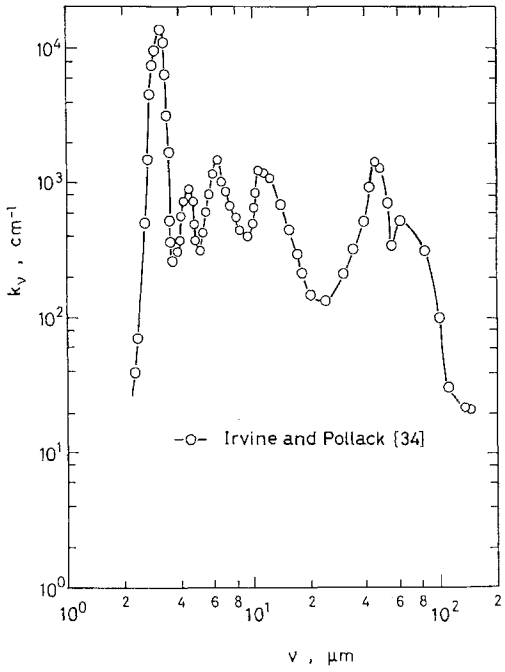

Fig. 7. Absorption coefficient of ice for long wavelengths.

3. THERMOPHYSICAL PROPERTIES OF SNOW

3.1. Thermal Conductivity of Snow

A number of determinations of the thermal conductivity of snow λ_s have been performed, usually with only a density measurement specifying the snow feature. The temperature ranges under which the data were obtained were usually not presented. The investigators gave an empirical relationship between thermal conductivity and density to indicate over limited density ranges. This information is summarized in Fig. 8 and Table I. The great scatter of the data in the figure appears to be due to the snow conditions such as aging and grain size, to the effect of mass diffusion, and to the measurement method for determining λ_s. Sawada et al. [42] determined the local thermal conductivity of naturally deposited snow layers. In the determination of the thermal conductivity, a temperature gradient is imposed, which subsequently results in a vapor gradient and then causes vapor-mass diffusion. Thus, the thermal

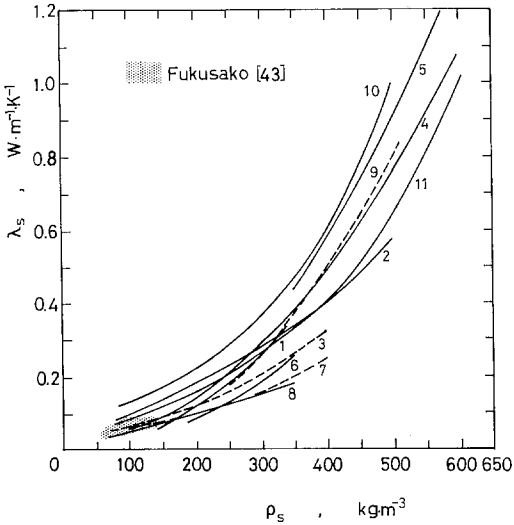

Fig. 8. Thermal conductivity of snow. Numbers denote the references given in Table I.

conductivity of snow includes essentially the mass diffusion. This indicates that the transient measurement method may be more accurate than the steady-state technique.

Most reported data have been obtained under the disturbed condition, namely, under the condition that snow was not only forced into a variety of boxes but also considerably aged. An *in situ* measurement of thermal

Table I. Relationships Between Thermal Conductivity ($W \cdot m^{-1} \cdot K^{-1}$) and Density ($kg \cdot m^{-3}$) of Snow

No.	Ref.	Expression	Density range
1	Abels [13]	$\lambda_s = 2.85 \times 10^{-6} \rho_s^2$	
2	Jansson [13]	$\lambda_s = 2.09 \times 10^{-2} + 7.96 \times 10^{-4} \rho_s + 2.51 \times 10^{-12} \rho_s^4$	80–500
3	van Dusen [13]	$\lambda_s = 2.09 \times 10^{-2} + 4.19 \times 10^{-4} \rho_s + 2.18 \times 10^{-9} \rho_s^3$	
4	Devaux [37]	$\lambda_s = 2.93 \times 10^{-2} + 2.93 \times 10^{-6} \rho_s^2$	100–600
5	Kondrat'eva [38]	$\lambda_s = 3.65 \times 10^{-6} \rho_s^2$	>350
6	Bracht [38]	$\lambda_s = 2.05 \times 10^{-6} \rho_s^2$	190–350
7	Yoshida and Iwai [39]	$\log \lambda_s = -1.47 + 2.0 \times 10^{-3} \rho_s$	72–400
8	Sulakvelidze [38]	$\lambda_s = 5.11 \times 10^{-4} \rho_s$	<350
9	Yen [40]	$\lambda_s = 3.22 \times 10^{-6} \rho_s^2$	
10	Izumi and Fujioka [41]	$\log \lambda_s = -1.17 + 2.16 \times 10^{-3} \rho_s$	80–500
11	Sakazume and Seki [7]	$\log \lambda_s = -1.25 + 2.12 \times 10^{-3} \rho_s$	150–700

conductivity of the new and undisturbed snow layer was carried out by Fukusako [43], who adopted the usual transient hot-wire method. A platinum wire 30 μm in diameter and 170 mm in length was horizontally stretched at the location of 25 mm from the bottom of an upper opened box whose capacity was 300 (length) $\times$ 200 (width) $\times$ 100 (depth) mm^3. Measurements were performed only when the snow in the box became greater than about 50 mm in depth during a 24-h period. The observed data for a disturbed show layer are shown in Fig. 11 by the shaded field. There seems to be still some scatter in the data, even for fresh snow.

The effect of temperature on λ_s has been examined by Pitman and Zuckerman [44] and Sakazume and Seki [7], whose data (their best-fitted lines) are graphically shown in Fig. 9. An inspection of the figure reveals that all the experimental data of Sakazume and Seki [7] decrease monotonically with increasing temperature at any prescribed density, while those of Pitman and Zuckerman [44] increase as the temperature

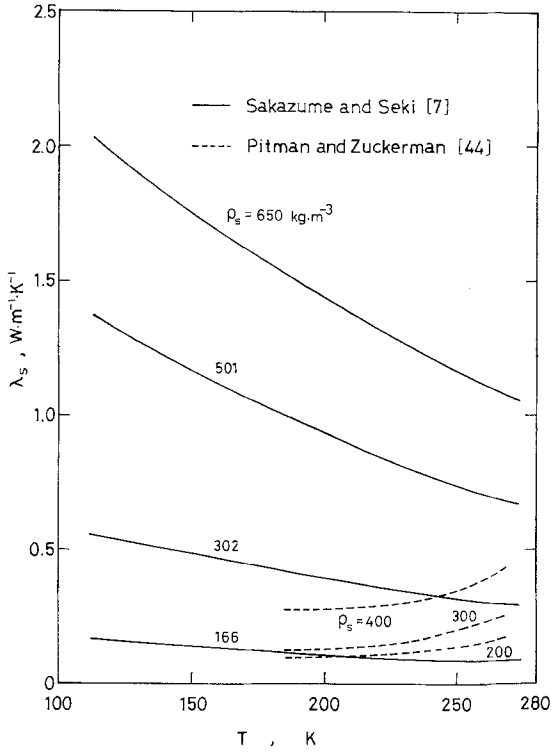

Fig. 9. Effect of temperature on the thermal conductivity of snow.

increases. The effect of temperature on λ_s found by Sakazume and Seki [7] appears to be more reliable considering that the transient Krisher's method was adopted by Sakazume and Seki.

3.2. Theoretical Model for Thermal Conductivity of Snow

A number of models have been derived to represent theoretically the thermal conductivity of snow. Woodside [45] adopted a model that considers the snow to be composed of a cubic lattice of uniform ice spherical particles in air, under the assumption that the air spaces are small enough so that heat transfer by convection may be neglected and that the isotherms are planes perpendicular to the direction of heat flow. Using Maxwell's work on the electrical conductivity of inhomogeneous media, Schwerdtfeger [46] derived theoretical expressions for the thermal conductivities of dense snow and light snow. For light snow, he utilized the spatial arrangement of the air space parallelipipeds within the ice medium to apply Maxwell's work on stratified conductors. Woodside's model was modified by Pitman and Zuckerman [44] so that it allows for thermal condition through continuous ice paths of thin cylindrical columns connecting all the spherical ice grains. Sakazume and Seki [7] correlated their experimental data by utilizing Russell's model [47], which was derived from the properties of its component gas and solid for a distribution of uniform pores of cubical shape arranged within a simple lattice.

Recently, adding the mass-diffusion effect to Pitman and Zuckerman's model, Maeno and Kuroda [48] determined the thermal conductivity of snow. Figure 10 shows the calculated results in which both $D_v = 2.1 \times 10^{-5}\ m^2 \cdot s^{-1}$ corresponding to the diffusion coefficient of water vapor through normal air and $D_v = 6.5 \times 10^{-5}\ m^2 \cdot s^{-1}$ for no mass flow (determined by Yen [49–51]) are adopted. Furthermore, the value of r/R is considered to be in general between 0.01 (fresh snow) and 0.2 (old and aged snow). In Fig. 10, the sphere of experimental data is denoted by the shaded field. It appears that all the experimental data are within the calculated bounds, indicating that the model by Maeno and Kuroda [48], which introduced an additional mass diffusion effect to Pitman and Zuckerman's model, reasonably describes the characteristics of the experimental data.

3.3. Specific Heat of Snow

Sakazume and Seki [7] determined the volumetric specific heat $(\rho C_p)_s$ of snow for temperatures ranging from 113 to 273 K and densities between

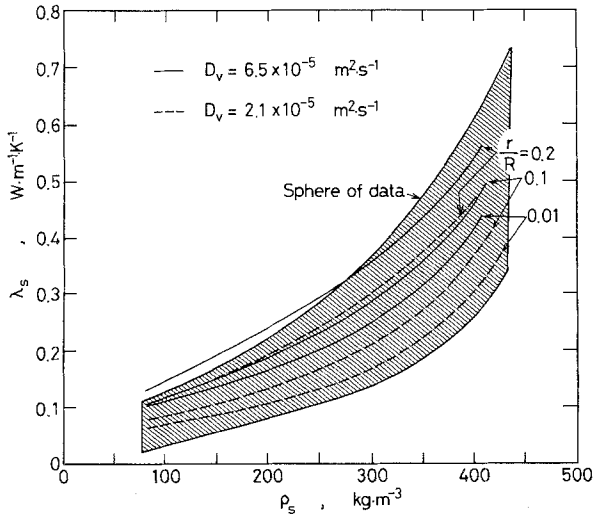

Fig. 10. Calculated results for the thermal conductivity of snow (Maeno and Kuroda [48]).

116 to 650 kg · m^{-3} using Krisher's method. Their experimental data for C_{p_s} reveal that the specific heat of snow is essentially identical to that of ice.

3.4. Thermal Diffusivity of Snow

The experimental data for the thermal diffusivity of snow were obtained by Devaux [37] (deduced by Maeno and Kuroda [48]) and Sakazume and Seki [7]. They noted that the thermal conductivity of snow was a function of temperature as well as density and increased with density.

4. THERMOPHYSICAL PROPERTIES OF SEA ICE

4.1. Characteristics of Sea Ice

Sea ice is a complex substance which is transformed to a complete solid mixture of pure ice and solid salts only at quite low temperatures. In general, when sea ice if maintained under its freezing point, pure ice crystals form, separating from the brine. As the freezing advances, pockets of brine are cut off, and the resulting ice is composed of pure ice, brine, solid salt crystals, and air bubbles. The equilibrium salt concentration of the brine which is trapped within the ice depends upon its temperature. Then when some temperature variations take place, the brine is concentrated or

diluted to a new equilibrium concentration by the formation of additional pure ice crystals or by the melting of pure ice. Thus, precise measurements of the thermophysical properties of sea ice always encounter considerable difficulties, because they are strongly dependent on temperature, salinity, and age; in fact it appears more reliable to use theoretical values based on a variety of models which have been developed for higher temperatures encountered in nature.

4.2. Thermal Conductivity of Sea Ice

The thermal conductivity is strongly dependent on the composition of sea ice, which can be specified by the density, salinity, and temperature. Thermal conductivity models for a sea ice were studied by Anderson [52], Langleben [53], Schwerdtfeger [54], and Horjen [55]. Neglecting the presence of air bubbles in sea water, Anderson [52] first considered the effect of the geometry of the brine inclusion on the bulk conductivity of the sea ice assuming the presence of brine in three different spatial configurations. Langleben [53] has shown that sea ice consisted of pure ice enclosing vertical cylinders of brine whose cross sections are elliptical and whose lengths are long compared with their average diameters at higher temperatures. By considering that sea ice essentially incorporates uniformly and randomly distributed spherical air bubbles, Schwerdtfeger [54] expanded Anderson's treatment. For an accreted ice layer, Horjen [55] adopted a model consisting of horizontal and vertical brine channels which have rectangular cross sections.

Compared with a number of theoretical models for the thermal conductivity of sea ice, very few measurements have been made. Sakazume and Seki [56] investigated the thermal conductivity of sea ice at lower temperature using Krisher's method, which appears to have a higher accuracy because the maximum temperature difference in a testing salt ice was less than 2°C. Figure 11 shows the experimental results for the thermal conductivity of sea ice as a function of temperature, along with those of Schwerdtfeger [54] and One [57]. It may be seen that the thermal conductivity at lower temperatures may be about 10% less than that of pure ice and decreases considerably with increasing temperature above −23°C. The λ_{si} for temperatures from −100 to −25°C can be reported as [56]

$$\lambda_{si} = 1.16(1.94 - 9.07 \times 10^{-2}\theta + 3.37 \times 10^{-5}\theta^2) \qquad (\mathrm{W \cdot m^{-1} \cdot K^{-1}};\ \theta,\ ^\circ\mathrm{C}) \tag{7}$$

The effect of fractional salt content S on the thermal conductivity is demonstrated in Fig. 12, where data obtained by Schwerdtfeger [54],

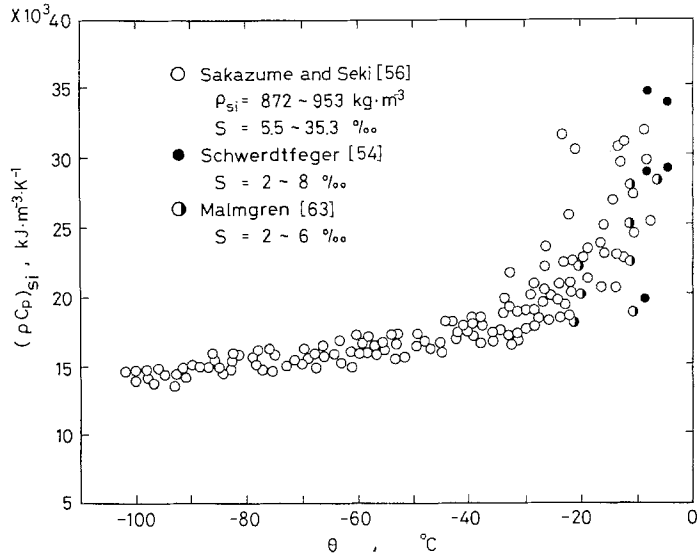

Fig. 11. Thermal conductivity of sea ice.

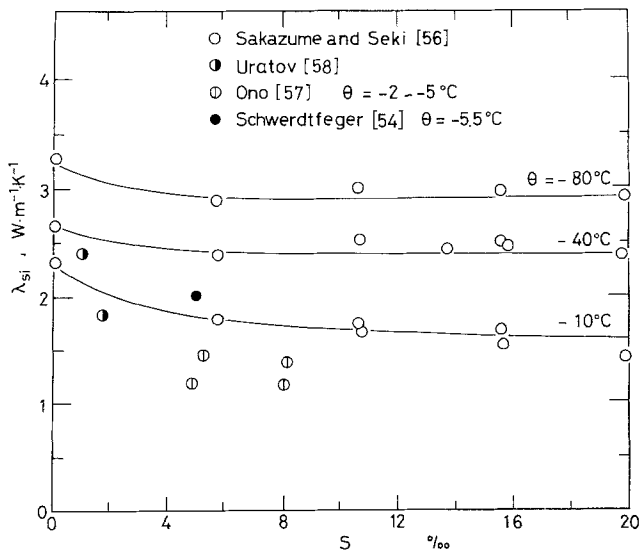

Fig. 12. Effect of salinity on the thermal conductivity of sea ice.

Sakazume and Seki [56], Uratov [58], and Ono [57] are shown. The figure indicates that the fractional salt content within sea ice may cause a decrease of the thermal conductivity compared with that of pure ice. However, it appears that at lower temperatures, the effect of the fractional salt content on thermal conductivity may become smaller since the sea ice is then composed of pure ice and solid salts.

4.3. Specific Heat of Sea Ice

The specific heat of sea ice is the total of both the heat required to raise the sea ice being composed of pure ice, brine, solid salt crystals, and air bubbles a unit of temperature and the heat associated with phase change. At temperatures not far from the freezing point sea ice has a large specific heat.

The phase diagram of seawater was given by Assur [59] based on the work of Nelson and Thompson [60]. The diagram indicates that above a temperature of $-8.2°C$ all salt trapped within the body of sea ice is essentially in solution. Between -8.2 and $-22.9°C$, the continuous precipitation of $Na_2SO_4\ 1OH_2O$ (sodium sulfate decahydrate) takes place. At $-22.9°C$, another hydrate, NaCl $2H_2O$, starts to precipitate.

When $\theta > -8.2°C$, the specific heat depends essentially upon both the relative extent of the phase change and the specific heat of pure ice and salt solution. Since the effects of heats of crystallization (or dilution) can be neglected based on data reported by Lange and Forker [61], Pounder [24] and Schwerdtfeger [54] gave the expression

$$C_{p_{si}} = -\frac{\sigma}{\alpha\theta^2} L_f + \frac{\sigma}{\alpha\theta}(C_{p_w} + C_{p_i}) + C_{p_i} \tag{8}$$

where α is the coefficient of the relationship between the fractional salt content of the brine S (in grams of salt per gram of water), σ is the salinity of sea ice (in grams of salt per gram of sea ice), and C_{p_w} and C_{p_i} are the specific heat of water and pure ice, respectively. From a somewhat different approach, One [62] proposed the following equation:

$$C_{p_{si}} = 4.187\left(0.505 + 0.0018\theta + 4311.5\frac{\sigma}{\theta^2} - 0.8\sigma + 0.20\sigma\theta\right)$$

$$(\mathrm{kJ \cdot kg^{-1}};\ \theta,\ °C) \tag{9}$$

Between -8.2 and $-22.9°C$ a continuous deposition of $Na_2SO_4\ 1OH_2O$ occurs. Assuming that the rate of precipitation of $Na_2SO_4\ 1OH_2O$ is linear, so that the quantity of deposition at any temperature can be estimated by extraporating from the initial section of the phase diagram of seawater, Schwerdtfeger [54] introduced another expression.

Sakazume and Seki [56] measured the cubic heat capacity $(\rho C_p)_i$ of sea ice using Krisher's method. In Fig. 13, their data are plotted along with those obtained by Malmgren [63] and Schwerdtfeger [54]. It is indicated in the figure that at lower temperatures the heat capacity of sea ice is 4 to 6% higher than that of the pure ice. This may due to the solid salts involved within sea ice. At temperatures higher than $-23°C$ the heat capacity increases sharply with temperature, as expected from Eq. (8).

4.4. Thermal Diffusivity of Sea Ice

The thermal diffusivity at high temperatures was calculated by Ono [64]. The experimental data for lower temperatures obtained by Sakazume and Seki [56] appear to be about 15% smaller than those for pure ice. As the temperature rises, λ_{si} decreases, while both ρ_{si} and C_{si} increase. Thus, the thermal diffusivity a_{si} shows a decrease that is more temperature dependent than any of its constituent parameters, particularly at temperatures near the freezing point.

4.5. Density of Sea Ice

Schwerdtfeger [54] and Cox and Weeks [65] considered theoretically the density of sea ice in detail. According to Cox and Weeks [65], the sea ice density is given by

$$\rho_{si} = (1 - v_a)/[1/\rho_i - S_i F_2(T)/F_1(T)] \quad (\mathrm{kg \cdot m^{-3}}) \tag{10}$$

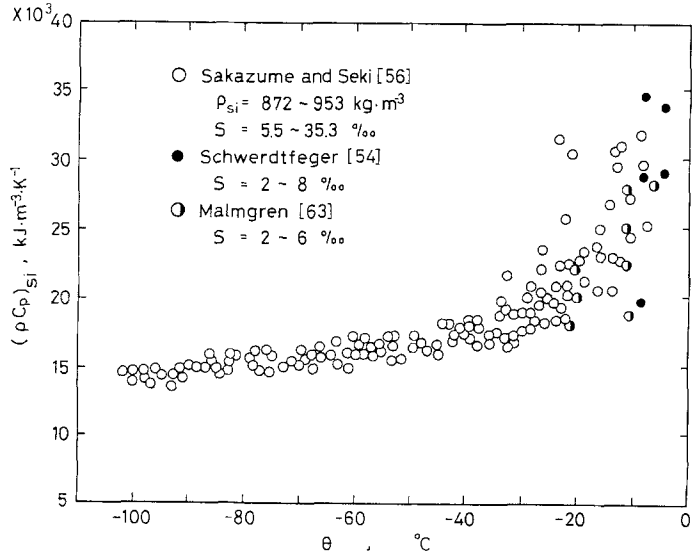

Fig. 13. Volumetric heat capacity of sea ice.

where v_a is the relative volume of air, ρ_i the density of the ice, S_i the salinity of the ice, and $F_1(T)$ and $F_2(T)$ are, respectively, expressed as

$$F_1(T) = \rho_b S_b (1 + \delta) \tag{11}$$

$$F_2(T) = [(1 + \gamma)\rho_b/\rho_i - \gamma\rho_b/\rho_{ss} - 1] \tag{12}$$

where ρ_b is the brine density, S_b the salinity of the brine, δ the ratio of the mass of salt in the brine to mass of salt in the solid salts, γ the ratio of the mass of solid salts to the mass of the brine, and ρ_{ss} the average solid salt density. Equation (10) indicates that the sea ice density at a prescribed salinity tends to increase slightly with an increase in temperature provided that the air content is constant.

4.6. Latent Heat of Fusion of Seawater

The latent heat of fusion L_{si} of sea ice is the amount of heat required to melt a unit mass of sea ice of salinity σ and temperature θ, because sea ice has no fixed temperature for phase change. Yen [33] initroduced the latent heat of fusion L_{si} by integrating the specific heat equation given by Ono [64] as follows:

$$L_{si} = 4.187\left(79.68 - 0.505\theta - 27.3\sigma + 4311.5\frac{\sigma}{\theta} + 0.8\sigma\theta - 0.009\theta^2\right)$$

$$[\mathrm{kJ \cdot kg^{-1}};\ \theta,\ ^\circ\mathrm{C}] \tag{13}$$

4.7. Thermal Expansion of Sea Ice

The coefficient of thermal expansion of sea ice was extensively investigated by Cox [66], who concluded that the coefficient of sea ice was equal to that of pure ice.

5. CONCLUDING REMARKS

A comprehensive review concerning the thermophysical properties of ice, snow, and sea ice has been presented. The available data for thermal conductivity, specific heat, latent heat of fusion, thermal expansion, and thermal diffusivity were shown graphically for easier practical use. Reproducible data for snow were found to be much more difficult to obtain, because snow starts to undergo a metamorphism as soon as it falls on the ground. All the thermal properties of sea ice were demonstrated to be functions of both salinity and temperature. It is noted that the specific heat of sea ice is in general much greater than that of normal ice, especially when the temperature approaches the fusion temperature of the normal ice.

ACKNOWLEDGMENT

It is a pleasure to acknowledge the help received from Mr. M. Tago during the preparation of the present paper. The author would like to thank him for his continuous interest, encouragement, and many illuminating discussions.

REFERENCES

1. R. W. Powell, *Adv. Phys.* 7:276 (1958).
2. J. K. Landauer and H. Plumb, SIPRE Research Paper 16 (1956).
3. M. Jakob and S. Erk, *Zh. Tekh. Fiz.* **10**:623 (1929).
4. E. H. Ratcliffe, *Phil. Mag.* 7:1197 (1962).
5. D. S. Dillard and K. D. Timmerhaus, *Pure Appl. Cryogen.* 4:35 (1966).
6. T. Ashworth, *Proc. 4th. Int. Cryogen. Eng. Conf.* (1972), p. 377.
7. S. Sakazume and N. Seki, *Bull. JSME* **44**(382):2059 (1978).
8. F. H. Schofield and J. A. Hall, *Int. Crit. Table* **2**:312 (1927).
9. M. S. van Dusen, *Int. Crit. Table* **5**:216 (1929).
10. J. Klinger, *J. Glaciol.* **14**:517 (1975).
11. J. W. Dean and K. D. Timmerhaus, *Adv. Cryogen. Eng.* **8**:263 (1963).
12. H. C. Dickinson and N. S. Osborne, *Bull. Bur. Stand. (U.S.)* **12**:49 (1915).
13. N. E. Dorsey, *Properties of Ordinary Water Substance* (Reinhold, New York, 1940).
14. W. F. Giauque and J. W. Stout, *J. Am. Chem. Soc.* **58**:1144 (1936).
15. P. Flubacher, A. J. Leadbetter, and J. A. Morrison, *J. Chem. Phys.* **33**:1751 (1968).
16. M. Sugisaki, H. Suga, and S. Seki, *Bull. Chem. Soc. Jap.* **41**:2591 (1968).
17. D. C. Ginnings and R. J. Corruccini, *J. Res. Natl. Bur. Stand.* **38**:583 (1947).
18. K. Lonsdale, *Proc. R. Soc.* **A247**:424 (1958).
19. G. Dantl and I. Gregora, *Naturwissenschaften* **55**:176 (1968).
20. D. Eisenberg and W. Kausmann, *The Structure and Properties of Water* (Oxford University Press, London, 1969), p. 296.
21. S. J. LaPlaca and B. Post, *Acta Crystallogr.* **13**:503 (1960).
22. P. V. Hobs, *Ice Physics* (Clarendon Press, Oxford, 1974), p. 348.
23. R. Brill and A. Tippe, *Acta Crystallogr.* **23**:343 (1967).
24. E. R. Pounder, *Physics of Ice* (Pergamon Press, New York, 1965).
25. R. L. Cameron and C. B. Bull, *Natl. Acad. Sci. Nat. Res. Council Pub.* **1036**:178 (1962).
26. D. W. James, *J. Mater. Sci.* 3:540 (1968).
27. A. W. Smith, *J. Opt. Soc. Am.* **10**:710 (1925).
28. F. D. Rossini, D. D. Wagman, W. H. Evens, S. Levine, and I. Jaffe, *NBS Circ.* **500**:126 (1952).
29. M. Jakob and S. Erk, *Z. Ges. Kalte-Ind.* **35**:125 (1928).
30. T. R. Butkovich, SIPRE Research Report 40 (1957).
31. G. Dantl, *Z. Phys.* **166**:115 (1962).
32. A. J. Leadbetter, *Proc. R. Soc.* **A287**:403 (1965).
33. Y. C. Yen, *CRREL Rep.* **81**:3 (1981).
34. W. M. Irvine and J. B. Pollack, *Icarus* **8**:324 (1968).
35. L. E. Goodrich, Tech. Paper No. 331, Div. Build. Res., Ottawa (1970).
36. N. Seki, S. Sugawara, and S. Fukusako, *Wärme- Stoffubertrag.* **11**:207 (1978).
37. J. Devaux, *Ann. Phys.* **20**:5 (1933).
38. M. Mellor, CRREL Monograph III-A1, AD611023 (1964).

39. Z. Yoshida and Y. Iwai, *Low Temp. Sci.* **A3**:79 (1950).
40. Y. C. Yen, *J. Geophys. Res.* **67**:1091 (1962).
41. K. Izumi and T. Fuzioka, *Low Temp. Sci.* **A33**:91 (1967).
42. S. Sawada, N. Seki, and S. Fukusako, *3rd Jap. Symp. Thermophys. Prop.* **3**:137 (1982).
43. S. Fukusako, *Proc. 1st Jap.-U.S. Joint Semin. Thermophys. Prop.* **1**:127 (1983).
44. D. Pitman and B. Zuckerman, *J. Appl. Phys.* **38**:2698 (1967).
45. W. Woodside, *Can. J. Phys.* **36**:815 (1958).
46. P. Schwerdtfeger, *IAHS-AISH Publ.* **61**:75 (1963).
47. H. W. Russel, *J. Am. Ceram. Soc.* **18**:1 (1935).
48. N. Maeno and T. Kuroda, in *Properties and Structures of Snow and Ice, Fundamental Glaciology Series 1* (Kokon Shoin, Tokyo, 1986).
49. Y. C. Yen, *J. Geophys. Res.* **68**:1093 (1963).
50. Y. C. Yen, *J. Geophys. Res.* **70**:1821 (1965).
51. Y. C. Yen, *J. Geophys. Res.* **72**:1283 (1967).
52. D. L. Anderson, *NAS-NRCPubl.* **598** (1958).
53. M. P. Langleben, *Bull. Am. Phys. Soc. Ser. 2* **5**:359 (1960).
54. P. Schwerdtfeger, *J. Glaciol.* **4**:789 (1963).
55. I. Horjen, *Proc. 1st Int. Symp. Cold Regions Heat Transfer* (1987), p. 115.
56. S. Sakazume and N. Seki, *Bull. JSME* **46**:1119 (1980).
57. N. Ono, *Low Temp. Sci.* **23**:167 (1965).
58. D. C. Uratov, *Prob. Arkt-Antarkt* **9**:79 (1961).
59. A. Assur, *U.S. Snow, Ice and Permafrost Res. Estab. Res. Rep. 44* (1960).
60. K. H. Nelson and T. G. Thompson, *J. Marine Res.* **13**:166 (1954).
61. N. A. Lange and G. M. Forker, *Handbook of Chemistry* (Sandusky, Ohio, 1952).
62. N. Ono, *Low Temp. Sci.* **24**:249 (1966).
63. F. Malmgren, *Norweg. No. Pola Exped. Maud. Sci. Res.* **1**:67 (1927).
64. N. Ono, *Low Temp. Sci.* **26** (1968).
65. G. F. N. Cox and W. F. Weeks, *J.Glaciol.* **29**:306 (1983).
66. G. F. N. Cox, *J. Glaciol.* **29**:425 (1983).